PERGAMON

Available online at www.sciencedirect.com
SCIENCE DIRECT®

International Journal of Rock Mechanics & Mining Sciences 40 (2003) 485–495

International Journal of
Rock Mechanics
and Mining Sciences

www.elsevier.com/locate/ijrmms

Modelling the size of the crushed zone around a blasthole

S. Esen[a,*], I. Onederra[a], H.A. Bilgin[b]

[a] Julius Kruttschnitt Mineral Research Centre, The University of Queensland, Brisbane, Qld, Australia
[b] Department of Mining Engineering, Middle East Technical University, Ankara, Turkey

Accepted 11 February 2003

Abstract

A new model to predict the extent of crushing around a blasthole is presented. The model is based on the back-analysis of a comprehensive experimental program that included the direct measurement of the zone of crushing from 92 blasting tests on concrete blocks using two commercial explosives. The concrete blocks varied from low, medium to high strength and measured 1.5 m in length, 1.0 m in width and 1.1 m in height. A dimensionless parameter called the crushing zone index (*CZI*) is introduced. This index measures the crushing potential of a charged blasthole and is a function of the borehole pressure, the unconfined compressive strength of the rock material, dynamic Young's modulus and Poisson's ratio. It is shown that the radius of crushing is a function of the *CZI* and the blasthole radius. A good correlation between the new model and measured results was obtained. A number of previously proposed models could not approximate the conditions measured in the experimental work and there are noted discrepancies between the different approaches reviewed, particularly for smaller diameter holes and low strength rock conditions. The new model has been verified with full scale tests reported in the literature. Results from this validation and model evaluations show its applicability to production blasting.

1. Introduction

For a number of years, both researchers and practising engineers have been aware of the importance of being able to tailor blast fragmentation to optimise the overall mineral extraction and recovery cycle. It is widely acknowledged that in production blasting a significant proportion of the fine material present in a muckpile originates from the zone of crushing produced during blasting. Predicting the extent of the crushing zone is important to practitioners interested in the modelling of the complete size distribution of fragments in blasting.

Fines can have a negative or positive impact on the efficiency of downstream processes. For example, the generation of excessive fines in operations adopting leaching as their main ore processing method, may hinder recovery as certain fines tend to affect the permeability of leaching pads. Leaching performance may be affected if the proportion of material that is less than 150 μm exceeds 12 percent in the feed to the agglomerators [1]. Similarly, the efficiency of coal processing is strongly related to the generation of fines of less than 0.5 mm. Increased fines content in run of mine (ROM) feed leads to higher handling and processing costs, low yields, increased product moisture content, and in many cases a reduced product value [2]. There is also evidence (e.g. [3]) to suggest that by providing an appropriate size distribution to crushing and grinding circuits, a measurable increased throughput and/or reduced power draw can be obtained. This may entail a requirement to increase the proportion of finer material in production blasting.

The need to be able to predict the amount of fines from blasting has driven the development of this new engineering model. The model developed in this study is based on a comprehensive experimental program conducted between 1996 and 1999 as part of a collaborative research project between the Middle East Technical University and the BARUTSAN explosives company in Ankara, Turkey [4]. One of the principal aims of this research project was to investigate the influence of the explosive, rock and blast design parameters on the

*Corresponding author. Julius Kruttschnitt Mineral Research Centre, University Mine Site, Isles Road, Indooroilly, Qld. 4068, Australia. Tel.: +61-7-3365-5888; fax: +61-7-3365-5999.
E-mail address: s.esen@mailbox.uq.edu.au (S. Esen).

1365-1609/03/$ - see front matter
doi:10.1016/S1365-1609(03)00018-2

efficiency of blasting. Tests were not limited to measuring the extent of crushing but also included measurements of breakage angle, breakage width, size distribution, throw, back-break, face velocity, minimum response time and peak particle velocity. In this study, the data set consisted of 92 model scale blasting tests. It is aimed to model the size of the crushed zone around a blasthole using this data set.

Model scale blasting experiments using synthetic materials (e.g. Plexiglass, Homolite 100, Epon 815 epoxy and concrete) have been used to understand the mechanisms of rock breakage by explosives and have provided very useful insights into the blasting process. This includes work conducted by Rustan and Vutukuri [5], Dick et al. [6], Fourney [7], Aimone-Martin et al. [8] and Raina et al. [9]. Studies by Dick et al. [6] and Stimpson [10] suggest that cement-based materials such as concrete can be used to simulate rocks. Applications largely arise from the cheapness, ease of fabrication and reproducibility of samples [10].

This paper gives a brief review of a selection of models discussed in the literature and describes the experimental program, the development of the new model and makes a comparison of the proposed approach with existing models.

2. A brief review of existing models

After detonation of the explosive, the whole blasthole is filled with gaseous detonation products at very high pressure and temperature. This pressure is exerted immediately on the wall of the blasthole, generating radial compressive stress, which is so much higher than the strength of the rock that a thin zone (Fig. 1) is formed around the blasthole in which the rock has yielded and been extensively broken or crushed by granular cracking, microcracking, differential compression of the particles and matrix of the rock and other forms of plastic deformation [11].

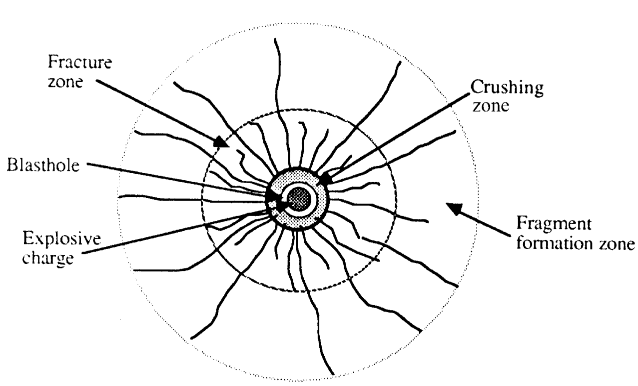

Fig. 1. Schematic illustration of processes occurring in the rock around a blasthole, showing formation of crushing zone, fracture zone and fragment formation zone [11].

Several models have been proposed for the estimation of the extent of crushing around a blasthole e.g. Il'yushin [12] and Vovk et al. [13] (documented by Hustrulid [14]), Szuladzinski [15], Djordjevic [16] and Kanchibotla et al. [17]. These approaches resolve explosive performance assuming ideal detonation and estimate the extent of the crushing zone using semi-empirical formulae. A brief description of each of these models is given in this section.

2.1. Il'yushin [12] and Vovk et al. [13]

The behaviour of the rock in the zone of fine crushing is described by Il'yushin [12] by assuming the model of an isotropic, incompressible granular medium with cohesion. In this case, the crushing zone radius, r_c (mm) is given by

$$r_c = r_o\left(\frac{P_b}{-(k/f) + [\sigma_c + (k/f)]L^{2f/(1+f)}}\right)^{1/2\gamma}\sqrt{L},$$

$$L = \frac{E/(1+\upsilon)}{\sigma_c[1+\ln \sigma_c/T]}, \tag{1}$$

where r_o is the borehole radius (mm), P_b is the borehole pressure (Pa), γ is the explosive's adiabatic expansion constant, k is the cohesion (Pa), f is the coefficient of internal friction, σ_c is the unconfined compressive strength (Pa), T is the tensile strength (Pa), E is the Young's modulus (Pa) and v is the Poisson's ratio. Borehole pressure is calculated by Eq. (A.3) in Appendix A.

The literature suggests that this model was limited to cases where the main mode of failure is compression and was mainly validated in high strength rock conditions. The equations were applied to talc-chlorite and limestone and it was noted by Vovk et al. [13] that they appeared to overestimate the extent of crushing.

2.2. Szuladzinski [15]

Szuladzinski [15] models the crushing and cracking in the proximity of a blasthole from transient dynamic analysis. The rock is modelled as an elastic body with an implied crushing capability and a definite cracking strength. The relationship proposed to estimate the radius of crushing, r_c (mm) is

$$r_c = \sqrt{\frac{2r_o^2\rho_o Q_{ef}}{F_c'}}, \tag{2}$$

where r_o is the borehole radius (mm), ρ_o is the explosive density (g/mm^3), Q_{ef} is the effective energy of the explosive (Nmm/g) assumed to be 2/3 of the heat of complete reaction (Nmm/g), and F_c' is the confined dynamic compressive strength of the rock material (MPa). F_c' is assumed to be approximately eight times the value of unconfined static compressive strength, σ_c (MPa).

2.3. Djordjevic [16]

This model is based on the Griffith failure criterion. The radius of crushing, r_c (mm) is given by

$$r_c = \frac{r_o}{\sqrt{24T/P_b}}, \tag{3}$$

where r_o is the radius of the blasthole (mm), T is the tensile strength of the rock material (Pa) and P_b is the borehole pressure (Pa). Borehole pressure is calculated by Eq. (A.3) in Appendix A.

2.4. Kanchibotla et al. [17]

This model estimates the radius of crushing as a function of the borehole radius, the detonation pressure and the unconfined compressive strength and it is given by the following relationship:

$$r_c = r_o\sqrt{\frac{P_d}{\sigma_c}}, \tag{4}$$

where r_o is the borehole radius (mm), P_d is the detonation pressure (Pa) and σ_c is the unconfined compressive strength of the rock (Pa). Detonation pressure is calculated by Eq. (A.2) in Appendix A.

A review on the application of this particular model suggests that the approach was not intended to give accurate predictions of the actual extent of crushing but was used instead as an empirical tool to determine a volume of fine material contributing to the run of mine blast fragmentation as discussed by Kanchibotla et al. [17] and Kojovic et al. [18].

In general, the accuracy of those models that calculate detonation or borehole pressure as input parameters can be questioned on the basis of their inherent assumption of ideal detonation behaviour. On the other hand, approaches which adopt assumed values of dynamic rock material properties derived from static values may also be affected by the lack of data supporting these relationships. Validation is also an issue that should be highlighted, as in the majority of cases, the radius of crushing cannot be directly measured and very few case studies appear to support model predictions.

The proposed new model is based on a comprehensive experimental program which allowed for the direct measurement of the radius of crushing in model scale blasting tests. In addition, the new approach is able to approximate real detonation behaviour using non-ideal detonation modelling, enabling the prediction of borehole pressure as a function of explosive and rock properties and blasthole diameter. A more detailed discussion of this methodology is given in Appendix A.

3. Experimental work

3.1. Sample preparation

As shown in Fig. 2, concrete blocks were rectangular in shape and measured 1.5 m in length, 1.0 m in width and 1.1 m in height.

Three concrete mix designs were prepared to obtain low, medium and high strength concrete types. Table 1 summarises the components used in 1 m^3 of concrete for each mixture. Sica FF was used in order to increase the workability of high strength concrete. Mix designs were adjusted after determining the moisture content of the aggregates.

Specially prepared mixes were poured into a steel mould arrangement which included a greased cylindrical steel pipe of a specified diameter. The steel pipe was placed at the centre of the mould and fixed at the desired burden distance from the front side of the mould and later removed to create the blasthole. All concrete blocks were left to cure for at least 28 days before testing.

Cylindrical concrete samples of 15×30 cm in size were tested to obtain physical and mechanical properties, including unit weight, unconfined compressive strength, splitting tensile strength, P and S-wave velocity, all in accordance with ASTM Standards [19]. In addition, non-destructive tests such as Rebound

Fig. 2. Concrete block samples [4].

Table 1
Material quantity for 1 m^3 of concrete [4]

Material	Amount (kg)		
	Low strength concrete	Medium strength concrete	High strength concrete
Cement	200	425	500
Water	126	192	95
0/3 mm aggregate	1393	807	897
5/15 mm aggregate	587	859	956
Sica FF	—	—	10

Table 2
Physical and mechanical properties of concretes [4]

Concrete		R	σ_c (MPa)	T (MPa)	ρ (kg/m^3)	V_P (m/s)	V_S (m/s)	E_d (GPa)	v_d
Low strength concrete	Min	15.9	6.7	0.3	2255	3372	1871	20.2	0.278
	Max	25.1	10.5	0.8	2271	3752	2064	24.8	0.283
Medium strength concrete	Min	29.6	16.3	1.2	2286	3935	2157	27.3	0.285
	Max	44.7	24.6	2.9	2379	4553	2471	37.5	0.291
High strength concrete	Min	39.5	42.1	2.2	2340	4341	2363	33.7	0.290
	Max	52.9	56.5	4.3	2456	4891	2642	44.4	0.294

R: Hammer rebound; σ_c: Uniaxial compressive strength; T: Splitting tensile strength; ρ: Density; V_P: P-wave velocity; V_S: S-wave velocity; E_d: Dynamic Young's modulus; v_d: Poisson's ratio.

Hardness and Ultrasonic Pulse Velocity were carried out. A summary of the range of measured physical and mechanical properties is given in Table 2.

3.2. Explosive properties

Properties of the commercial explosives used in the experimental work are summarised in Table 3.

Because charge lengths were small in these particular tests, the confined velocity of detonation (VOD) was not measured directly. However, independent unconfined and confined VOD tests were conducted for all the commercial explosives (dynamites and ANFO type explosives) used in the research project. These measurements were used to determine the confined VOD for each test by adopting the following relationship developed by Esen [20]:

$$D_{\text{confined}} = \alpha q_n^{\beta} D_{\text{unconfined}}^{\varphi} \left(\frac{E_d}{1 + v_d} \right)^{\omega}, \tag{5}$$

where α, β, φ and ω are constants; D_{confined} is the confined VOD (m/s); q_n is the heat of reaction for non-ideal detonation (MJ/kg); $D_{\text{unconfined}}$ is the unconfined VOD of an explosive at a given charge diameter (m/s); E_d is the dynamic Young's modulus (GPa) and v_d is the dynamic Poisson's ratio.

3.3. Test parameters and data collection procedures

During the tests, factors such as confinement, explosive type, specific charge, burden distance, blasthole diameter and decoupling ratio were varied one at a time. A summary of the range of parameters used in the experimental work is given in Table 4.

Each test blast was instrumented with a triaxial arrangement of high frequency geophones and monitored with the use of a high-speed video camera. After each test, the extent of crushing, breakage angle, breakage width, the overall fragment size distribution, throw, back-break, face velocity, minimum response time and peak particle velocity were measured.

Table 3
Properties of explosives [4]

	Gelatin dynamite	Elbar 1 dynamite
Density (g/cm^3)	1.5	1.0
Heat of reaction (MJ/kg)	4.70	3.76
Ideal VOD (m/s)	7527	5070
Ideal detonation pressure (GPa)	23.71	8.29
Unconfined VOD of 16 mm charge (m/s)	1278	1081

4. Data analysis and model development

As indicated earlier, several post-blast results were documented and analysed from the research project conducted in Ankara, Turkey [4]. This paper focuses on the development of a model to predict the radius of crushing for a given charge configuration and geotechnical condition. The objective of the work was also to produce a model that would include rock material and explosive input parameters that could be easily obtainable and are generally available in mining operations. This would ensure the applicability of the model in production blasting applications.

As discussed by Whittaker et al. [11], the compressive strength and stiffness characteristics of the rock material play a major role in the development of the zone of crushing or zone of plastic deformation. As the process of crushing is dynamic, a crushing zone model should include dynamic rock material properties. However, many of these dynamic properties cannot be directly measured and are not readily available, resulting in the use of assumed multipliers. For example, Szuladzinski [15] assumes the dynamic confined compressive strength to be 8 times the value of unconfined compressive strength. Mohanty and Prasad [21] give an insight into the dynamic strength characteristics of rock materials at strain rates similar to those experienced during blasting. Using the Split Hopkinson Bar they suggest that the ratio of the unconfined dynamic strength to static values of unconfined compressive strength ranged between 2.5 and 4.6 for 12 rock types.

Table 4
Blast design parameters for fully coupled and decoupled model scale tests

Parameter	Fully coupled tests	Decoupled tests
Explosive	Gelatin dynamite, Elbar 1 dynamite	Elbar 1 dynamite
Decoupling ratio[a]	1	1.25, 1.50, 1.75, 2.00
Blasthole diameter (mm)	16–20	20, 24, 28, 32
Burden (cm)	22.7–46.2	18.2–31.3
Hole depth (cm)	40.4–45.4	39.8–45.0
Specific charge (kg/m^3)	0.110–0.250	0.150–0.175
Explosive amount (g)	8.0–22.8	7.8–16.1
Stemming material	1.18–3 mm aggregate	1.18–3 mm aggregate
Stemming length (cm)	26.5–40.3	21.0–39.6
Stemming length/burden	0.67–1.47	0.69–2.18
Burden/blasthole diameter	14.2–28.9	6.5–15.4
Initiation system	Electric detonator	Electric detonator
Confined VOD[b] (m/s)	1901–2600	—
Borehole pressure[b] (GPa)	1.002–1.469	0.470–0.940

[a] Decoupling ratio = borehole diameter/charge diameter where charge diameter is 16 mm for decoupled blast tests.
[b] Detonation velocity and borehole pressure are computed by the non-ideal detonation model developed by Esen [20].

As indicated earlier, the approach adopted in this study was to include both static and dynamic properties that are readily available. Hence, the extent or radius of crushing denoted as r_c shown in Fig. 3 was assumed to be a function of explosive type, material properties and borehole diameter.

As shown by Fig. 3, r_o is the original borehole radius (mm), P_b is the borehole pressure (Pa) calculated using non-ideal detonation theory, K is the rock stiffness (Pa) and σ_c is the uniaxial compressive strength (Pa). Rock stiffness K is defined assuming that the material within the crushing zone is homogeneous and isotropic and is given by

$$K = \frac{E_d}{1 + \upsilon_d}, \tag{6}$$

where E_d is the dynamic Young's modulus and v_d is the dynamic Poisson's ratio. If the dynamic Young's modulus E_d is not available, it may be estimated from knowledge of the static value by the following relationship [22]:

$$\log_{10} E_{st} = 0.02 + 0.77 \log_{10}(\gamma E_d), \tag{7}$$

where E_{st} is the static Young's modulus (GPa) and γ is the density (g/cm^3).

Crushing takes place under a triaxial state of compression. In this study, uniaxial compressive strength is taken into account because it is easily obtainable and generally available at most mining and quarrying operations.

Borehole pressure is computed from the non-ideal detonation model developed by Esen [20], which is briefly discussed in Appendix A.

Given the above measurements and calculations and by applying dimensional analysis, two dimensionless indices (π_1 and π_2) were derived:

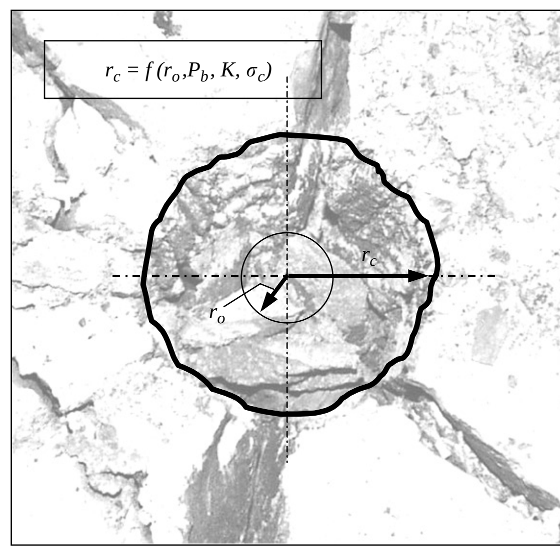

Fig. 3. Parameters influencing the extent of crushing.

$$\pi_1 = \frac{r_o}{r_c} \tag{8}$$

and

$$\pi_2 = \frac{(P_b)^3}{(K) \times \sigma_c^2} \text{ or crushing zone index } (CZI), \tag{9}$$

where as noted earlier, r_c is the crushing zone radius (mm), r_o is the borehole radius (mm), P_b is the borehole pressure (Pa), K is the rock stiffness (Pa) and σ_c is the uniaxial compressive strength (Pa).

The relationship between the two indices given above is shown in Fig. 4. The function obtained by non-linear

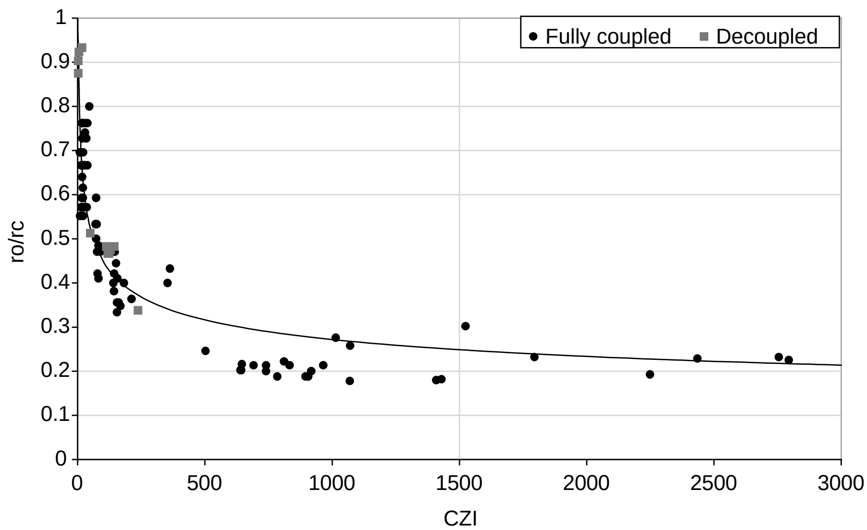

Fig. 4. Relationship between CZI and r_o/r_c for 92 model scale test blasts.

regression is given by

$$\frac{r_o}{r_c} = 1.231(CZI)^{-0.219} \tag{10}$$

or

$$r_c = 0.812 r_o (CZI)^{0.219}, \tag{11}$$

where CZI is defined as the crushing zone index. This is a dimensionless index that identifies the crushing potential of a charged blasthole. The correlation coefficient of the relationship given by Eq. (10) is $R^2 = 0.83$. The CZI appears to capture the dynamic process taking place in the crushing zone by taking into account both explosive (borehole pressure) and rock properties (uniaxial compressive strength and stiffness) as well as borehole radius.

Because it is physically impossible for the ratio between r_o and r_c to be greater than 1, the relationship (Eq. (10)) is constrained to 1 for very small values of CZI, in this case for values of CZI of less than 2.6. These small values of CZI will generally correspond to small borehole pressures (i.e. decoupled charges and/or very high strength rock/low energetic explosive couple). The 92 data points shown in Fig. 4 clearly cover a wide range of conditions for which ratios of r_o/r_c can be obtained.

5. Comparison of the new approach with existing models

In this section, the proposed approach is compared with predictions given by the models reviewed in Section 2. A comparison is conducted using experimental data from the model scale blasting experiments. In addition, a comparison is made between the models for several geotechnical conditions and blasthole diameters found in full scale blasting environments.

5.1. *Comparison of models against experimental data from model scale tests*

Fig. 5 shows a comparison of plots of the measured size of the crushing zone against predicted values for all the models considered. The new model developed in this study predicts the size of the crushing zone with reasonable accuracy. However, the other models could not approximate the conditions in the experimental work. Szuladzinski's [15] predictions are closer to the new model than the approaches proposed by Il'yushin [12] and Vovk et al. [13], Djordjevic [16] and Kanchibotla et al. [17]. One of the possible reasons is that these models assume ideal detonation which is not valid for the model scale tests. Explosives show a more pronounced non-ideal detonation behaviour under these conditions.

5.2. *Relative comparison of models in full scale blasting conditions*

As a way of comparing the predictive capabilities of the models under full scale blasting conditions, a number of simulations were carried out for the geotechnical conditions summarised in Table 5. The analysis included two different explosive types, namely ANFO and water resistant ANFO denoted as WR ANFO and a range of blasthole diameters (51–229 mm). The results are summarised in Table 6.

In general, all the models follow the expected trends; for example, for a specific material property and explosive type, as the blasthole diameter increases the crushing zone radius increases. Similarly, the models show that an explosive with the capacity to generate higher borehole pressures has the potential to increase crushing for the same blasthole diameter and material

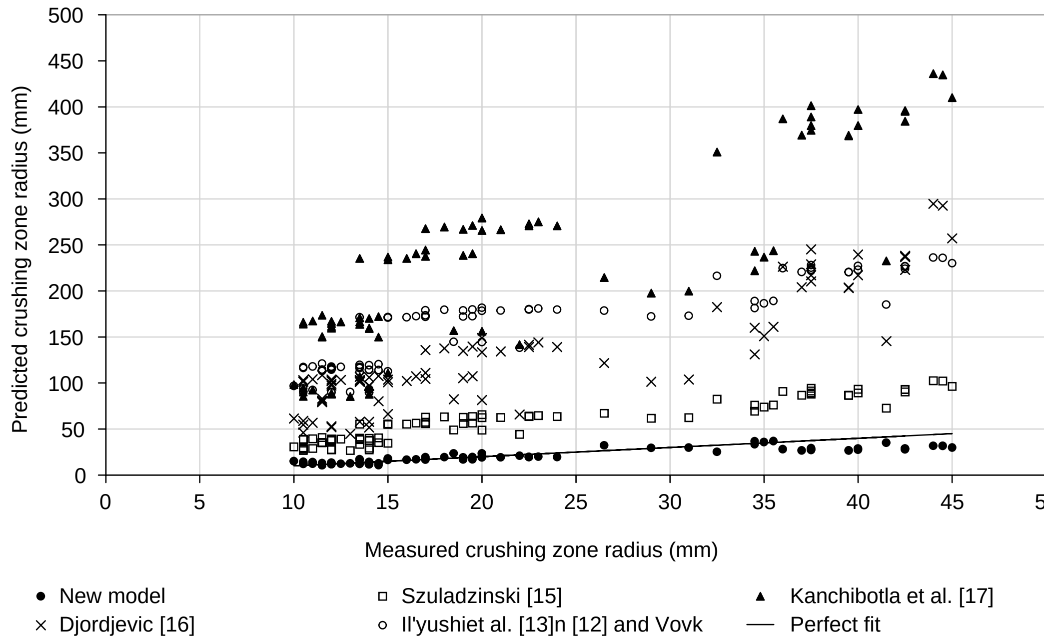

Fig. 5. Comparison of all models in reduced scale blasting experiments.

Table 5
Physical and mechanical properties of rock types used in the simulations [4]

Rock	σ_c (MPa)	T (MPa)	ρ (kg/m^3)	E_d (GPa)	v_d
Clayey-limestone	24.2	3.3	2256	23.5	0.243
Basalt	114.0	14.2	3000	95.8	0.298

property. There are notable discrepancies between the different models, as shown in Table 6. This is more pronounced in small diameter blastholes and low strength rock types.

The new model shows that the ratio between the crushing zone radius and the borehole radius (r_c/r_o) is a function of explosive, rock properties and blasthole diameter. For the simulations listed in Table 6, the range of r_c/r_o is between 1.3 and 6.6. Hustrulid [14] has indicated that the assessments of the size of the crushing zone are conflicting. However, he suggests that most investigators hold the view that the r_c/r_o ratio does not exceed 3–5 borehole radii, which is in agreement with the ranges predicted in the simulation results shown in Table 6.

Under these simulated conditions (Table 6), the analysis shows that Szuladzinski's [15] and Djordjevic's [16] estimations are closer to the new approach than the models proposed by Il'yushin [12] and Vovk et al. [13] and Kanchibotla et al. [17]. As discussed earlier, it is fair to note that those models that adopt a measure of borehole pressure and assume ideal detonation for its calculation may overestimate the radius of crushing. The new approach considers the effect of the non-ideal behaviour of commercial explosives in the calculation of borehole pressure as discussed in Appendix A.

6. Verification of the applicability of the model to full scale blasting

The radius of crushing cannot be directly measured in a full scale production environment because the rock is fragmented and displaced after the detonation of the explosive charge. In order to validate and verify the applicability of a model to predict the extent of crushing around a blasthole, single hole blast experiments must be specifically designed. These particular tests rely on the willingness of operations to disrupt normal production activities at a very high cost. Because of these issues and due to resource constraints, the authors were unable to implement such tests. Nevertheless, full scale tests reported by Olsson and Bergqvist [23] and Slaughter [24] have been used to verify model predictions and its applicability to full scale blasting.

The tests conducted by Olsson and Bergqvist [23] were used to verify the capability of the model to predict the size of the crushed zone from decoupled charges in granite. In this case study, a 64 mm diameter hole was

Table 6
Relative comparison of crushing zone models in full scale blasting conditions

Blasting domain	Explosive	Explosive density (g/cm^3)	Heat of reaction q (MJ/kg)	D_{CJ} (km/s)	Hole diameter (mm)	Hole radius r_o (mm)	Charge radius r_e (mm)	Borehole pressure P_b (GPa)	r_c* (mm) new model	r_c (mm) [12,13]	r_c (mm) [15]	r_c (mm) [16]	r_c (mm) [17]	Ratio r_c^*/r_o
Clayey-limestone	ANFO	0.803	3.812	5.016	165	82.5	82.5	3.045	372	1269	379	466	1192	4.5
Clayey-limestone	ANFO	0.803	3.812	5.016	229	114.5	114.5	3.477	564	1761	526	647	1654	4.9
Basalt	ANFO	0.803	3.812	5.016	102	51.0	51.0	2.061	67	402	108	139	339	1.3
Basalt	ANFO	0.803	3.812	5.016	165	82.5	82.5	3.148	143	651	175	225	549	1.7
Basalt	ANFO	0.803	3.812	5.016	229	114.5	114.5	3.595	217	903	242	312	762	1.9
Clayey-limestone	WR ANFO	0.994	3.918	5.829	51	25.5	25.5	2.016	88	441	132	186	476	3.5
Clayey-limestone	WR ANFO	0.994	3.918	5.829	102	51.0	51.0	4.033	277	881	264	372	953	5.4
Clayey-limestone	WR ANFO	0.994	3.918	5.829	165	82.5	82.5	4.974	513	1426	427	602	1541	6.2
Clayey-limestone	WR ANFO	0.994	3.918	5.829	229	114.5	114.5	5.440	756	1979	593	836	2139	6.6
Basalt	WR ANFO	0.994	3.918	5.829	51	25.5	25.5	2.085	34	239	61	90	219	1.3
Basalt	WR ANFO	0.994	3.918	5.829	102	51.0	51.0	4.169	107	478	122	179	439	2.1
Basalt	WR ANFO	0.994	3.918	5.829	165	82.5	82.5	5.141	198	774	197	290	710	2.4
Basalt	WR ANFO	0.994	3.918	5.829	229	114.5	114.5	5.623	291	1074	273	403	985	2.5

charged with a 22 mm diameter packaged explosive charge (Gurit). Very short cracks around the borehole and a negligible crushing zone were observed.

The newly proposed model calculates the ratio of crushing zone radius to borehole radius to be 1.0; that is, almost no crushing takes place. Thus, the results from the new model and blasting tests conducted in granite are in good agreement. However, the methods of Il'yushin [12] and Vovk et al. [13], Djordjevic [16] and Kanchibotla et al. [17] predict a crushing zone radius of 62, 33 and 122 mm, respectively. Djordjevic's [16] model is the only other method that appears to effectively consider the effect of decoupling. Szuladzinski's [15] approach does not take into account the decoupling effect. For this particular comparison, all models adopted the Nie [25] adjustment of borehole pressure for horizontal decoupling (see Appendix A).

Slaughter [24] conducted a program of field investigations in the area of coal fines generation. The size of the crushed zone was measured in blasts where ANFO and blend type explosives were detonated in coal at the Coal and Allied's Hunter Valley Mine. Direct measurements were taken by digging a trench after each test hole. The blasthole diameter used was 160 mm. Average coal properties used in the modelling are a uniaxial compressive strength of 20 MPa [24] and an assumed stiffness of 6.65 GPa. Table 7 shows the comparison of the measured and predicted radii of crushing.

Although the newly proposed model underestimates the size of the crushed zone resulting from the detonation of the ANFO charge, it appears to predict the radius of crushing well for the emulsion charges. These discrepancies may be due to the modelled explosive behaviour and assumed rock properties (stiffness). Nevertheless, the model captures the relative trends and shows that the use of a higher energetic explosive charge (Emulsion) can result in a much larger crushed zone than with lower energetic explosive (ANFO). If the blastholes are dry, it would therefore be appropriate to select ANFO in order to reduce the amount of coal fines resulting from the crushing zone.

7. Conclusions

A new engineering model to predict the extent of crushing around a blasthole has been presented. The strength of this model lies in the comprehensive experimental program conducted, which allowed the direct measurement of the extent of crushing for a wide range of conditions in concrete blocks. A total of 92 test blasts were analysed and used in its development. A good correlation between model and measured results was observed.

The new model shows that the ratio between the crushing zone radius and borehole radius (r_c/r_o) is a

Table 7
Comparison of the measured and predicted radii of crushing in coal blasting

Explosive	Explosive density (g/cm^3)	Detonation velocity (m/s)	Borehole pressure (GPa)	Measured radius of crushing zone(m)	Predicted radius of crushing zone(m)
ANFO	0.81	4077	2.929	0.67	0.48
Emulsion	1.20	5364	6.878	0.76	0.84
Emulsion	1.20	5364	6.878	0.83	0.84

function of explosive type, rock properties and blasthole diameter.

In general, the model follows the expected trends; for example, for a specific rock environment and explosive type, as the blasthole diameter increases the crushing zone radius increases. Similarly, the model shows that an explosive with the capacity to generate higher borehole pressures has the potential to increase crushing for the same blasthole diameter and rock environment.

A number of previously proposed models could not approximate the conditions measured in the experimental work and there are noted discrepancies between the different reviewed approaches, particularly in smaller diameter holes and low strength rock conditions.

The new model has been verified with full scale tests reported in the literature. Results from this validation and model evaluations show its applicability to production blasting.

The proposed approach can be directly applied as an engineering tool to estimate the amount of fines generated during production blasting in both surface and underground operations. For example, the radius of crushing may be used to define a volume of crushed rock around individual blastholes.

Acknowledgements

The authors would like to acknowledge the support of the BARUTSAN Explosives Company, Turkey. Many thanks go to Muharrem Kilic, Nedim Yesil and BARUTSAN Co. staff and technicians. The authors would also like to thank Prof. E.T. Brown, Prof. B. Whiten, Dr. R. Trueman and Dr. G. Chitombo of the Julius Kruttschnitt Mineral Research Centre (JKMRC) for their suggestions.

Appendix A. Determination of borehole pressure

Borehole pressure describes the expansion work of the explosive during the rock breakage process. This data directly indicates the transfer of the explosive energy into the rock and hence is a direct measure of the efficiency of the explosives. Therefore, it is the most important information in an evaluation of the explosive performance and the prediction of blasting results. Despite the importance of this parameter, direct measurements of the borehole pressure have rarely been carried out due to the absence of feasible methods, instead, various empirical formulas or detonation theories are used to estimate it. However, the accuracy of such estimates remains unknown [25].

This Appendix is not aimed at reviewing detonation theories, but ideal and non-ideal detonation theories are explained briefly to clarify the pressure concept used in the crushing zone models.

Determination of the detonation pressure by ideal detonation theory

Ideal detonation assumes the following [26]: the flow is one-dimensional; the plane detonation front is a jump discontinuity, a shock in which the chemical reaction is assumed to be completed; and the jump discontinuity is steady (independent of time).

The ideal (CJ) detonation criterion requires that there is one steady solution, the CJ point. The CJ state relations are given in literature by Fickett and Davis [26] and Mader [27]. Particularly the CJ detonation pressure is

$$P_{CJ} = \frac{\rho_o D_{CJ}^2}{\gamma + 1}, \tag{A.1}$$

where P_{CJ}, D_{CJ}, ρ_o and γ are the CJ detonation pressure (Pa), CJ detonation velocity (m/s), density of the unreacted explosive (kg/m^3) and specific heat ratio, respectively. The assumption $\gamma = 3$ gives the well-known expression [28]:

$$P_{CJ} = \frac{\rho_o D_{CJ}^2}{4}. \tag{A.2}$$

The detonation pressure should not be confused with the borehole or explosion pressure, which is the pressure of the explosive gases expanded to the initial volume of the borehole. The borehole pressure is thus equal to the pressure of the reaction products after the reaction has gone to completion in a constant volume. This pressure is often referred to as the constant volume explosion pressure, or simply explosion pressure [29].

Borehole pressure is theoretically about 45% of the detonation pressure assuming complete reaction at the detonation front. It is not easy to define the borehole pressure for the non-ideal explosives since the time for completion of the reaction may well extend far into the period of large expansion of the borehole [29].

According to Persson et al. [28], borehole pressure, P_b (Pa), for a fully coupled hole can be estimated through

$$P_b = \frac{P_{CJ}}{2}. \quad (A.3)$$

Determination of the detonation pressure by non-ideal detonation theory

It has been established that commercial explosives exhibit non-ideal detonation behaviour since detonation velocity strongly depends on charge diameter and confinement [28–34].

Non-ideal behaviour of explosives can be explained by applying the two-dimensional detonation theory. Some of the methodologies and/or models in the literature have been developed by Wood and Kirkwood [35]; Bdzil [36]; Chan [37], Kirby and Leiper [38]; Bdzil and Stewart [39]; Bdzil and Stewart [40]; Lee [41]; Souers [42], Deng et al. [43] and Esen [20].

In this study, the model developed by Esen [20] is used to predict the explosive performance and compute the borehole pressure for the new crushing zone model. Esen [20] developed a non-ideal detonation code based on the Souers [42] model. Since Souers [42] model resolves two-dimensional detonation theory for the unconfined case, it has been extended by Esen [20] to include the confinement effect on explosive performance. Esen [20] treated the non-ideal detonation problem as an engineering problem and developed a systematic engineering methodology to solve it.

Inputs to the model include the heat of complete reaction, CJ detonation velocity (these two parameters are calculated using an ideal detonation code), density of the explosive, charge diameter, dynamic Young's modulus and dynamic Poisson's ratio of the rock medium (which describe confinement). The model uses experimental unconfined VOD and charge diameter data for a given explosive. The non-ideal detonation model then computes the confined detonation properties including a pressure–volume diagram. Esen [20] determines the pressure–volume diagram by using the following equation:

$$P = \frac{\frac{1}{2}\left(D^2 - u^2\right) + q_n\left(10^6\right)}{V\left(1/(\gamma - 1) + 1\right)}, \quad (A.4)$$

where P is the pressure (Pa); D is the non-ideal detonation velocity (m/s); u is the particle velocity (m/s); V is the specific volume (m^3/kg); γ and q_n are specific heat ratio and heat of complete reaction (MJ/kg), respectively for non-ideal case.

Borehole pressure is determined when volume ratio, V/V_o is 1.0 where V_o is $1/\rho_o$.

The model has shown to estimate the confined detonation velocity within a reasonable error for dry blasting agents [20].

Borehole pressure in a decoupled blasthole

The decoupled borehole pressure is given by [25,44]

$$(P_b)_{dc} = P_b\left(\sqrt{C}\frac{r_e}{r_b}\right)^a, \quad (A.5)$$

where $(P_b)_{dc}$ is the decoupled borehole pressure (Pa), P_b is the fully coupled borehole pressure (Pa), C is the percent of the hole loaded with explosive. C is a factor that accounts for vertical decoupling. When the explosive is loaded continuously along the axis of the hole as it is in the case of our experiments, $C = 1$. r_e is the charge radius (mm), r_b is the borehole radius (mm) and a is the constant which is determined as 2.6, 2.4 and 2.0 by Atlas Powder [45], Workman and Calder [44] and Nie [25], respectively. In this study, $a = 2.0$ is used.

References

[1] Scott A, David D, Alvarez O, Veloso L. Managing fines generation in the blasting and crushing operations at Cerro Colorado Mine. Proceedings of the Mine to Mill 1998 Conference. The Australasian Institute of Mining and Metallurgy, Brisbane, Australia, 1998. p. 141–8.

[2] Djordjevic N, Esterle J, Thornton, D, La Rosa D. A new approach for prediction of blast induced coal fragmentation. Proceedings of the Mine to Mill 1998 Conference. The Australasian Institute of Mining and Metallurgy, Brisbane, Australia, 1998. p. 175–81.

[3] Grundstrom C, Kanchibotla SS, Jankovich A, Thornton D. Blast fragmentation for maximising the sag mill throughput at Porgera Gold Mine. Proceedings of the 27th Annual Conference on Explosives and Blasting Technique, vol. 1. ISEE, Orlando, FL, USA, 2001. p. 383–99.

[4] Bilgin HA, Esen S, Kilic M. Patarge Project, Internal Report, Barutsan A.S., Elmadag, Ankara, Turkey, 1999 [in Turkish].

[5] Rustan A, Vutukuri VS. The influence from specific charge, geometric scale and physical properties of homogeneous rock on fragmentation. Proceedings of the First International Symposium on Rock Fragmentation by Blasting, Lulea, Sweden, 1983. p. 115–42.

[6] Dick RD, Fourney WL, Wang XJ, Young C. Results from instrumented small scale tests. Proceedings of the Fourth International Symposium on Rock Fragmentation by Blasting-Fragblast-4, Vienna, Austria, 1993. p. 47–54.

[7] Fourney WL. Mechanisms of rock fragmentation by blasting. Comprehensive Rock Engineering Principles, Practice and Projects, vol 4. Oxford: Pergamon Press, 1993. p. 39–69.

[8] Aimone-Martin CT, Dick RD, Weaver TA, Edwards CL. Small Scale cratering expereriments I: concrete. FRAGBLAST—Int J Blasting Fragmentation 1998;2;:143–80.

[9] Raina AK, Chakraborty AK, Ramulu M, Jethwa JL. Rock mass damage from underground blasting, a literature review, and lab- and full scale tests to estimate crack depth by ultrasonic method. FRAGBLAST—Int J Blasting Fragmentation 2000;4:103–25.

[10] Stimpson B. Modelling materials for engineering rock mechanics. Int J Rock Mech Min Sci Geomech Abstr 1970;7:77–121.

[11] Whittaker BN, Singh RN, Sun G. Rock fracture mechanics principles, design and applications, Amsterdam: Elsevier, 1992. p. 444–5 [Chapter 13].
[12] Il'yushin AA. The mechanics of a continuous medium. Izd-vo MGU. Moscow. (Translated in Hustrulid W. Blasting principles for open pit blasting, vol. II. Rotterdam: Balkema, 1999. p. 964–1009 [Chapter 21]), 1971 [in Russian].
[13] Vovk A, Mikhalyuk A, Belinskii I. Development of fracture zones in rocks during camouflet blasting. Sov Min Sci 1973;9(4):383–7.
[14] Hustrulid W. Blasting principles for open pit blasting, vol. II. Rotterdam: Balkema, 1999. p. 964–1009 [Chapter 21].
[15] Szuladzinski G. Response of rock medium to explosive borehole pressure. Proceedings of the Fourth International Symposium on Rock Fragmentation by Blasting-Fragblast-4, Vienna, Austria. 1993. p. 17–23.
[16] Djordjevic N. Two-component of blast fragmentation. Proceedings of the Sixth International Symposium on Rock Fragmentation by Blasting-Fragblast 1999, South African Institute of Mining and Metallurgy, Johannesburg, South Africa. 1999. p. 213–9.
[17] Kanchibotla SS, Valery W, Morrell S. Modelling fines in blast fragmentation and its impact on crushing and grinding. Proceedings of Explo'99—A Conference on Rock Breaking. The Australasian Institute of Mining and Metallurgy, Kalgoorlie, Australia, 1999. p. 137–44.
[18] Kojovic T, Kanchibotla SS, Poetschka NL, Chapman J. The effect of blast design on the Lump:Fines ratio at Marandoo iron ore operations. Proceedings of the Mine to Mill Conference, The Australasian Institute of Mining and Metallurgy, Brisbane, Australia, 1998. p. 149–52.
[19] Annual Book of ASTM Standards. vol 04.02. 1992.
[20] Esen S. Modelling non-ideal detonation behaviour of commercial explosives. Internal Report, JKMRC, Australia, 2001.
[21] Mohanty B, Prasad U. Degree of rock fragmentation under high strain rates. Proceedings of the 27th Annual Conference on Explosives and Blasting Technique, vol. 2. Orlando, FL, USA: ISEE, 2001. p. 89–95.
[22] Eissa EA, Kazi A. Relation between static and dynamic Young's Moduli of rocks. Int J Rock Mech Min Sci Geomech Abstr 1988;25(6):479–82.
[23] Olsson M, Bergqvist I. Crack lengths from explosives in multiple hole blasting. Proceedings of the Fifth International Symposium on Rock Fragmentation by Blasting, Fragblast-5, Montreal, Quebec, Canada, 1996. p. 187–91.
[24] Slaughter S. Investigation of coal fines. Internal Report, JKMRC, Australia, 1991.
[25] Nie S. Measurement of borehole pressure history in blast holes in rock blocks. Fragblast 1999, South African Institute of Mining and Metallurgy, Johannesburg, South Africa, 1999. p. 91–7.
[26] Fickett W, Davis WC. Detonation. Berkeley: University of California Press, 1979. p. 16, 54.
[27] Mader CL. Numerical modeling of explosives, propellants. Florida, USA: CRC Press LLC, 1998. p. 3.
[28] Persson P, Holmberg R, Lee J. Rock blasting and explosives engineering. Florida, USA: CRC Press, 1993. p. 101, 106, 107.
[29] Hopler RB. Blasters' handbook. Cleveland, OH, USA: ISEE, 1998. p. 43.
[30] Leiper GA, Plessis MP. Describing explosives in blast models. Proceedings of the Second International Symposium on Rock Fragmentation by Blasting, Keystone, CO, USA, 1987. p. 462–74.
[31] Brinkmann JR. An experimental study of the effects of shock, gas penetration in blasting. Proceedings of the Third International Symposium on Rock Fragmentation by Blasting. Brisbane, Australia, 1990. p. 55–66.
[32] Udy L. Use of high density ammonium nitrate in blasting. Sixth High-Tech Seminar, vol. 1. Blasting Analysis International, Inc., Boston, USA. 1995. p. 415–21.
[33] Esen S. Ideal detonation behaviour of commercial explosives, development of an explosive/rock interaction model. M.Sc. thesis, Middle East Technical University, Ankara, Turkey, 1996. p. 61.
[34] Bilgin HA, Esen S. Assessment of ideality of some commercial explosives. Proceedings of the 25th Conference on Explosives and Blasting Technique, vol. 1. Nashville, TN, USA: ISEE, 1999. p. 35–44.
[35] Wood WW, Kirkwood JG. Diameter effect in condensed explosives. J Chem Phys 1954;22:1920–4.
[36] Bdzil JB. Steady-state two-dimensional detonation. J Fluid Mech 1981;108:195–226.
[37] Chan SK. A theory to predict the velocity-diameter relation of explosives. Proceedings of the Seventh International Symposium on Detonation, Annapolis, MD, USA, 1981. p. 589–601.
[38] Kirby IJ, Leiper GA. A small divergent detonation theory for intermolecular explosives. Proceedings of the Eighth International Symposium on Detonation, Albuquerque, 1985. p. 176–86.
[39] Bdzil JB, Stewart DS. Time-dependent two-dimensional detonation: the interaction of edge rarefactions with finite-length reaction zones. J Fluid Mech 1986;171:1–26.
[40] Bdzil JB, Stewart DS. Modeling two-dimensional detonations with detonation shock dynamics. Phys Fluids 1989;A1(7):1261–7.
[41] Lee J. Detonation shock dynamics of composite energetic materials. Ph.D. thesis, New Mexico Institute of Mining and Technology, USA, 1990.
[42] Souers PC. Size effect and detonation front curvature. Propell Explos Pyrot 1997;22:221–5.
[43] Deng J, Nie S, Nyberg U, Ouchterlony F. A burning model for five emulsion explosives and some applications, SveBeFo Report 43, Stockholm, 1999.
[44] Workman JL, Calder PN. Wall control blasting at the Manassas Quarry. Proceedings of the 18th Conference on Explosives and Blasting Technique, vol. 1. Orlando, FL, USA, 1992. p. 243–53.
[45] Atlas Powder. Explosive, rock blasting.Atlas Powder Company, Dallas, TX, USA, 1987. p. 200.